Introduction to Additive Manufacturing
Metal Additive Manufacturing

Jeanne Lee Cherng Yi
Dalia Somekh
Agasthya Vivek
Anastasia Meijer
Manuel Pascual Fernández

Wednesday 26th November, 2025

Supervising professors: Boillat Eric, Brugger Jürgen, Moser Christophe

1 Introduction

Additive manufacturing (AM) has transformed modern production by enabling geometries unattainable with conventional methods, reducing material waste, and eliminating the need for tooling. Although AM initially gained traction for rapid prototyping, the introduction of metal-capable processes in the 1980s—most notably Selective Laser Sintering and early powder bed fusion variants—marked a turning point in its industrial adoption. Since then, metal additive manufacturing has expanded dramatically with the development of Laser Powder Bed Fusion (L-PBF), Direct Energy Deposition (DED), and Electron Beam Powder Bed Fusion (EB-PBF), allowing the fabrication of high-performance components across aerospace, energy, medical, and consumer-product sectors.

Today, metal AM technologies are no longer experimental; they are widely deployed for applications ranging from mass-produced consumer electronics to safety-critical aerospace hardware. However, these successes are built on techniques whose fundamental operating principles have remained largely unchanged for decades. As a result, the next wave of progress in metal AM now focuses not on inventing new base processes, but on enhancing and extending existing ones through improved materials, sensing, automation, and laser technologies.

This report therefore concentrates on emerging developments that are shaping the future of **metal** additive manufacturing. First, advances in L-PBF are surveyed, including new printable alloys, refined scanning strategies, and innovations in melt-pool management. Building on this, we examine recent progress in *in-situ monitoring*, *machine-learning-enabled process interpretation*, and *adaptive control* for L-PBF, which together aim to transform it from a fixed-parameter process into an intelligent and self-correcting manufacturing system. The report then explores innovations in Wire Arc Additive Manufacturing (WAAM), a DED-based method gaining traction for large-scale metal components. This is followed by an overview of multi-material metal AM, highlighting its potential for functionally graded structures and hybrid-property components. Finally, cutting-edge laser wavelength technologies are discussed, with emphasis on how new beam colors and power-scaling strategies expand the range of processable metals.

Together, these topics illustrate how metal AM is evolving toward higher performance, greater reliability, and broader industrial capability through a combination of material science, sensing, machine intelligence, and photonics innovation.

2 Progress and Emerging Trends in Laser Powder Bed Fusion

Written by Jeanne Lee Cherng Yi

Laser Powder Bed Fusion (L-PBF) has become one of the dominant additive manufacturing (AM) techniques for producing metallic components with complex geometries and high mechanical performance. It is widely used in aerospace (lightweight brackets), biomedical implants (patient-specific prostheses), automotive components, energy and tooling applications, where conventional manufacturing would be too expensive or geometrically restrictive. This chapter discusses the recent advances in L-PBF, focusing on material developments and technical innovations in the process that aim to improve productivity and part quality.

2.1 Overview of the L-PBF Process

In order to identify potential improvements, we must first understand the L-PBF process. L-PBF manufactures parts layer by layer from a metallic powder. The powder is selectively consolidated by a laser beam moved by galvanometric mirrors (Figure 1). The consolidation occurs through local fusion or liquid phase sintering.

One of the main challenges of the process is its extreme thermal conditions: high cooling rates (10^4–10^6 K/s), steep thermal gradients, melt-pool instabilities, keyholing, and residual stresses, all of which can introduce defects such as porosity, cracking, or anisotropic microstructures. Powder quality, laser scan strategy, shielding gas flow, and machine architecture therefore play critical roles in determining the reliability and properties of the final components.

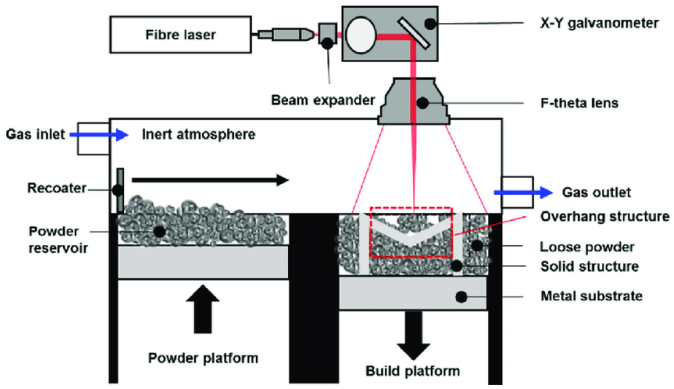

Figure 1: Schematic illustration of the laser powder bed fusion (L-PBF) process [1].

2.2 New Alloys for L-PBF: HEAs and SMAs

Traditionally, L-PBF has been used to manufacture alloys such as stainless steels, aluminium alloys and even Ti6Al4V. Yet, recent years we are starting to see the development of novel alloy systems tailored for AM, especially High-Entropy Alloys (HEAs) and Shape Memory Alloys (SMAs).

2.2.1 High-Entropy Alloys (HEAs)

HEAs are defined as alloys composed of five or more principal elements with near-equimolar concentrations (5–35 at.% each). Microstructurally, many HEAs form single-phase solid solutions with high-symmetry structures (bcc, fcc, or hcp) [2]. HEAs are attracting strong interest for molds, dies, turbine blades, hard coatings on cutting tools, and components in nuclear systems due to their excellent high-temperature strength, high fatigue resistance, balanced strength–ductility behavior, superconductivity, and exceptional irradiation resistance [3].

A frequent occurring challenge in the L-PBF fabrication of HEAs is cracking, a phenomenon caused by great thermal stresses from rapid cooling. High laser power when not controlled properly can increase the thermal stresses and promote hot cracking. Despite these challenges, recent studies have shown promising printability with HEAs:

- Niu et al. manufactured an AlCoCrFeNi HEA with a high relative density of 98.4% using L-PBF [4].
- Agrawal et al. demonstrated that L-PBF-processed FeMnCoCrSi had no cracking, with only 0.1 vol% porosity, and an ϵ-dominated columnar microstructure that significantly improved work-hardening and produced a very high strength–ductility index [5].

2.2.2 Shape Memory Alloys (SMAs)

SMAs are another emerging L-PBF alloy family. SMAs are known for their temperature-dependent mechanical response and their ability to recover strain when subjected to thermal cycling. This makes them well suited for biomedical devices, such as self-expanding cardiovascular stents, as well as actuators and adaptive structures. The most prominent SMA is NiTi. It is valued for its high damping capacity, corrosion resistance, and low density. Thanks to these properties, NiTi is also used in earthquake damping systems and vibration control in bridges.

Lu et al. fabricated NiTi using L-PBF and achieved a shape memory recovery ratio of 98.7% and 4.99% recoverable strain after 10 loading–unloading cycles [6]. This study demonstrates the feasibility of producing functional SMAs via L-PBF.

2.3 Advances in the L-PBF Process

Apart from developments in alloy design, continuous progress has also been made to improve the L-PBF process itself. These advances aim to improve part quality and process productivity, while addressing critical issues such as residual stresses, thermal gradients, melt-pool instability, and defect formation. This section focuses on recent findings on remelting strategies, multi-laser systems, spatter-control strategies, and powder recycling.

2.3.1 Remelting strategies

Remelting is an approach where the same powder layer is scanned multiple times during L-PBF (Figure 2). Remelting has become a widely used strategy to enhance part quality, particularly in terms of density and surface finish. As an in-situ heat treatment, remelting reduces steep thermal gradients and modifies the solidification conditions by decreasing the temperature gradient (G) and adjusting the cooling rate/solidification rate ratio (R). This stabilizes the melt pool, lowers residual stress, and delays or suppresses crack initiation, especially in alloys sensitive to hot cracking, such

as tungsten, Ni-based superalloys, and several HEAs. Consequently, this scanning approach is especially promising for alloys that exhibit poor printability in standard L-PBF conditions.

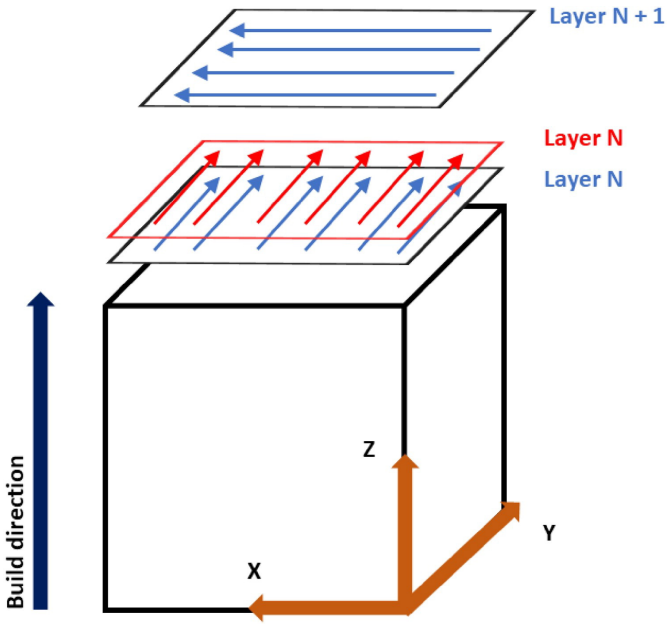

Figure 2: Illustration of remelting during L-PBF [7].

Studies have shown that [8] remelting tungsten by L-PBF have significantly reduced the grain size and defects in the material. Another study by Yu et al [9] further demonstrated that by remelting in the same direction reduces porosities than remelting in opposite scan direction. Remelting is closely linked to developments in scan strategy optimization. Scanning patterns such as stripes, chessboard or island patterns (Figure 3) directly affect residual stresses and melt-pool dynamics [10]. Studies also suggested that reducing scan vector length, implementing bidirectional scanning, and rotating scan strategies between layers can reduce warping and improve dimensional accuracy.

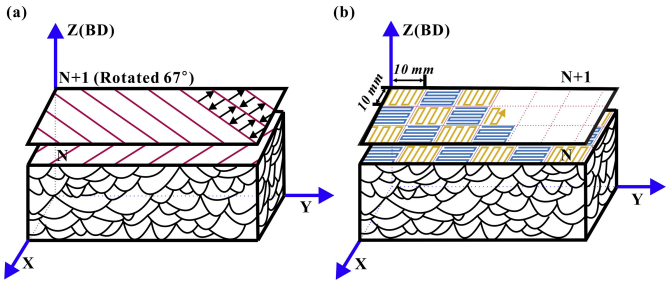

Figure 3: Illustration of scanning strategies (a) Stripes and (b) Chessboard [11].

2.3.2 Multi-laser systems

Multi-laser systems in L-PBF is one of the most impactful advances for industrial scalability. Manufacturers significantly boost productivity while enabling more flexible scanning approaches by employing multiple lasers. For instance, Wong et al. concluded that multi-laser setups can increase build rates without compromising density or significantly modifying the microstructure

of parts [12]. This is especially pertinent for large aerospace or energy-sector components where single-laser systems become time-consuming. Additionally, multiple lasers allow the use of different laser spot sizes for distinct geometrical regions. Fine features require high resolution whereas bulk regions benefit from larger, energy-efficient spots.

Besides adding laser units, Tsai et al. proposed a more compact solution: using a diffractive optical element and a galvanometric scanner to split a single laser into multiple simultaneously scanning beams. This approach preserves machine simplicity while enabling the adjustment of individual spot characteristics [13]. Such innovations suggest new opportunities for achieving high productivity without dramatically escalating machine cost.

2.3.3 Tackling the spattering phenomenon

In L-PBF, shielding gases are introduced to limit oxidation and avoid contamination of the material. Shielding gas is indispensable for preventing oxidation and controlling the build environment. However, it can unintentionally contribute to spatter formation (Figure 4), a critical issue in L-PBF. Spatter particles include:

- Cold spatter: unmelted powder displaced by gas flow.
- Hot spatter: molten droplets ejected from the melt pool.
- Recondensed particles: condensate that forms from metal vapor and settles onto the powder bed.

Zhang et al. [14] examined how gas flow influences the removal of melt-pool emissions. They found that the flow tends to move downward, which reduces its effectiveness. To address this issue, they added an extra row of gas nozzles beneath the existing ones which significantly improved spatter removal rate from 69% to 93%. Pauzon et al. [15] also studied how the thermal conductivity and heat capacity of shielding gases affect the density of Ti6Al4V parts produced by L-PBF. Instead of using pure argon, they experimented with mixtures of helium and argon, taking advantage of helium's higher thermal conductivity and heat capacity. Their results showed that using the gas mixture allowed the build rate to increase by up to 40% while maintaining process stability and achieving fully dense parts. The improved performance is attributed to more efficient spatter removal and enhanced cooling, even at higher laser powers and scanning speeds.

While the strategies above address spattering from a process-engineering perspective, emerging approaches based on in-situ monitoring and machine learning provide powerful alternatives; an extended discussion of these methods can be found in Chapter 3.

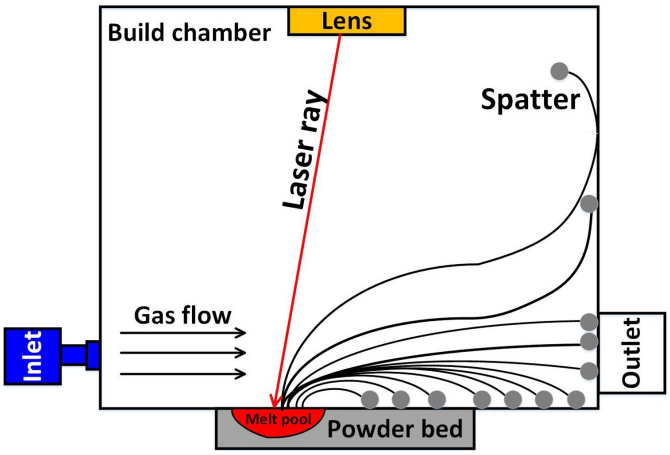

Figure 4: Schematic of the LPBF process chamber highlighting spatter behaviour and gas–flow interactions [14].

2.3.4 Powder recycling

Because the production of high-quality L-PBF powder is costly, the ability to reuse powder without degrading part quality is a crucial research topic. However, repeated exposure to the harsh thermal and chemical environment of L-PBF can alter powder characteristics through: Evaporation–condensation cycles which produce oxide films and increased oxygen content; Spatter contamination, causing the presence of large, irregular particles; Powder-size distribution (PSD) narrowing, causing loss of fine particles through sieving or vaporization.

Carrion et al. revealed that Ti6Al4V powders reused for 15 cycles showed improved flowability due to narrower PSD, yet the printed parts did no show significant changes in microstructure, tensile strength, or fatigue behaviour [16]. Moreover, Sutton et al. found similar PSD narrowing in 304L stainless steel but detected an increase in oxygen content and microstructural changes after seven cycles [17]. Lastly, Cordova et al. also observed oxygen content doubled in AlSi10Mg after 6 cycles, which can negatively affect ductility [18].

Not all alloys respond to recycling the same way. A research done by Wang et al. reported that CoCrW powders reused six times resulted in reduced mechanical performance, suggesting that alloy chemistry strongly influence recyclability [19].

To reduce degradation of part quality, industries adopt powder refresh strategies, by blending 12–22% virgin powder into recycled batches, in addition to strict sieving protocols to remove oversized spatter particles [20].

3 Process Monitoring and Adaptive Control in Laser Powder Bed Fusion

Written by Dalia Somekh

Building on the overview of the L-PBF process presented in the previous section, we now focus on the mechanisms that drive defect formation and the emerging strategies used to detect and mitigate these defects during fabrication. As noted earlier, the extreme thermal conditions of L-PBF can lead to several types of defects if melting and solidification are not properly controlled. Traditional quality assurance relies on post-build inspections such as CT scanning or metallography, which can identify defects but offer no possibility for intervention during the build.

To overcome this "build-then-inspect" limitation, recent research has introduced a new approach based on three elements: *in-situ monitoring*, *machine-learning-based interpretation of sensor data*, and *closed-loop process control*. Modern L-PBF systems can integrate optical, thermal, photodiode, or acoustic sensors that continuously capture information about melt pool behavior and powder-laser interaction. These signals can be processed with machine learning models to detect or predict instabilities, enabling real-time adjustments to laser power, scan speed, or re-scan strategies. In industry, manufacturers such as EOS, SLM Solutions, Renishaw, and GE Additive already offer in-situ monitoring modules, though these are currently used mainly for quality documentation rather than automated corrective control.

L-PBF is chosen as the focus of this section because it is the metal AM process with the most extensive research on sensing, data-driven modeling, and adaptive control. Studying these developments highlights how the process can evolve from fixed-parameter, open-loop operation toward a more robust, intelligent, and self-correcting manufacturing system.

3.1 Mechanisms of Defect Formation & Monitoring

For in-situ monitoring and control strategies to be effective, it is essential to understand how defects form in L-PBF and how these defects reveal themselves through measurable process signals. Guillén *et al.* [21] classify L-PBF defects according to their physical origin, linking them to melt pool behavior, powder spreading, and the extreme thermal conditions of the process. These defects fall into four main categories: geometrical, surface-quality, microstructural, and mechanical. Recognizing the mechanisms behind these defects also clarifies which physical phenomena must be monitored during the build. Key indicators include melt pool geometry, thermal gradients, plume behavior, layer surface topography, and even acoustic emissions. These signals form the basis for both defect detection and real-time corrective actions in advanced monitoring and control systems.

3.1.1 Geometrical/Dimensional Defects

Geometrical and dimensional defects arise from improper build setup, recoater-related issues, or deviations in layer thickness. Because such defects are typically attributable to operator error or inadequate machine calibration rather than intrinsic LPBF process physics, we do not examine them further here. In the context of this study, we assume correct machine setup and stable recoating conditions, allowing us to focus on defect mechanisms that stem directly from melt pool dynamics, thermal behavior, and laser-material interaction.

3.1.2 Surface-Quality Defects

Surface defects often serve as early indicators of melt pool instability or energy mismanagement:

Balling. Balling is a Plateau-Rayleigh instability in which the melt track breaks into spheres due to insufficient wetting or excessive scan speed [22]. This leads to poor track continuity and rough surfaces. Figure 5 shows increasing severity with higher scan speed.

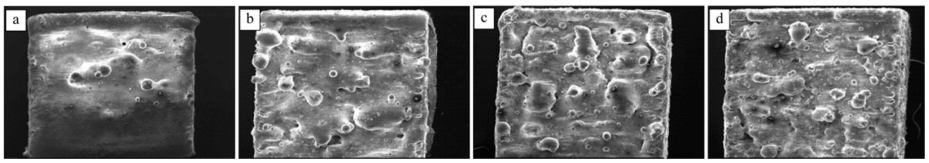

Figure 5: Balling severity increases with scan speed: (a) 250 mm/s, (b) 500 mm/s, (c) 750 mm/s, (d) 1000 mm/s [21].

Surface oxidation. Surface oxidation occurs when the melt pool is exposed to oxygen due to insufficient inert gas shielding or high temperatures that intensify vapor activity. Even small oxygen levels promote stable oxides, which modify absorptivity and surface tension, destabilizing the melt pool and promoting defects [23]. Early-stage oxidation can sometimes be mitigated by increasing laser power, slowing the scan, or applying a re-scan, but once thicker oxides form or chamber oxygen is elevated, the defect is no longer correctable.

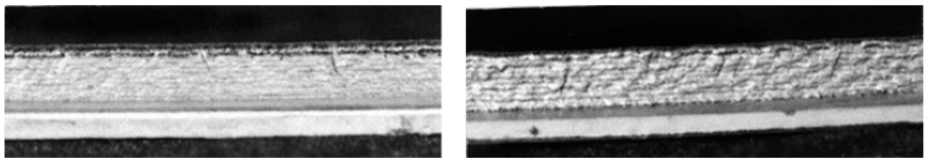

Figure 6: Slight oxidation (left) and severe oxidation (right) [21].

Surface roughness. Surface roughness forms when unstable melt tracks or spatter redeposition create local surface asperities, shown in Figure 7, often due to insufficient wetting or partial melting of surrounding powder [21]. Early-stage roughness can sometimes be reduced by applying a local re-scan or adjusting laser power.

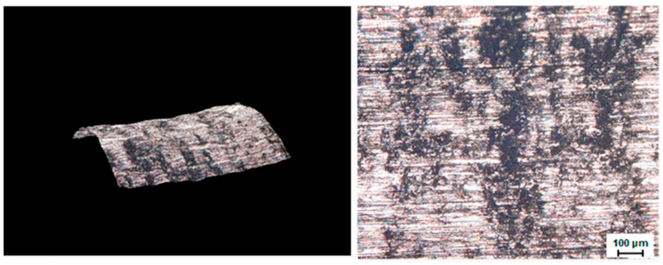

Figure 7: Example of surface roughness generated by spatter redeposition and melt-track instability [21].

Denudation. Denudation occurs when intense vapor-driven gas flow around the melt pool sweeps powder away from the scan track, leaving a depleted region with insufficient powder for proper melting [23]. This local powder deficiency can destabilize melt pool geometry and promote defects in subsequent layers.

Vaporization defects. Excessive laser energy causes intense metal vaporization, generating a high-velocity plume (metal vapor jet) that disturbs surrounding powder and increases spatter activity. These effects can initiate keyhole instability and further defect formation.

3.1.3 Microstructure Defects (Porosity)

Porosity refers to unintended voids formed within the solidified material. Unlike the intrinsic microscopic porosity associated with powder packing, these defects originate from unstable melt pool dynamics and improper energy input during the LPBF process. Such pores can severely reduce fatigue life and mechanical reliability, making their detection and mitigation essential.

Gas porosity. Gas porosity consists of small spherical voids formed by entrapped shielding gas or powder-bed gases during melting. These pores are typically found between partially melted powder particles, as shown in Fig. 8. While usually less severe than other porosity types, increased plume activity or high scan speeds can increase their formation. In-situ monitoring using photodiodes or cameras can detect elevated spatter or plume fluctuations associated with gas entrapment, enabling parameter adjustments.

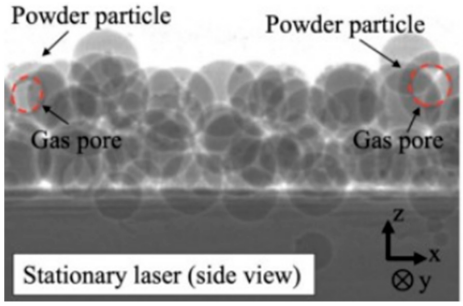

Figure 8: Example of gas pores trapped between partially melted powder particles under a stationary laser [21].

Keyhole porosity. Keyhole porosity arises when excessive laser energy creates a deep vapor cavity (keyhole) that becomes unstable and collapses, trapping gas in the solidifying metal [24]. These pores are typically large and spherical, as illustrated in Fig. 9. Since keyhole formation has strong optical and thermal signatures (intense plume emission, high photodiode response, and elevated melt pool temperature) it can often be detected in real time. Closed-loop control can reduce laser power or increase scan speed to stabilize the keyhole regime and mitigate further porosity formation.

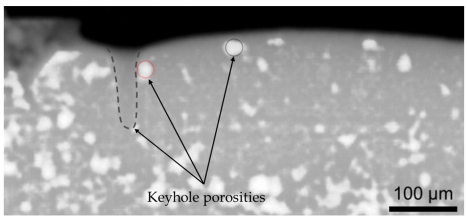

Figure 9: Keyhole-induced spherical pores created by collapse of an unstable vapor depression in LPBF [21].

Lack-of-fusion (LoF) porosity. LoF porosity forms when energy density is insufficient to fully melt the powder layer or fuse it with the underlying layer, resulting in irregular, crack-like voids [25]. Figure 10 shows typical LoF defects, which are highly detrimental because they act as stress concentrators. In-situ monitoring can identify LoF precursors such as abnormally low melt pool temperatures, reduced track brightness, or discontinuous melt pool shapes.

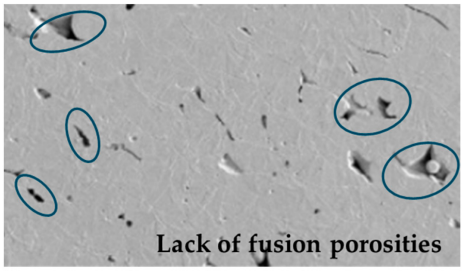

Figure 10: Irregular lack-of-fusion pores caused by insufficient energy input during LPBF [21].

3.1.4 Mechanical Defects

The extremely high cooling rates (10^4–10^6 K/s) and steep thermal gradients in L-PBF generate significant residual stresses within the material. These stresses can lead to cracking and inter-layer separation, especially in alloys with narrow solidification ranges or poor ductility at high temperatures.

Liquation cracking. Liquation cracking happens when some regions near the grain boundaries partially melt and then solidify again. Because these regions are weak while they are still half-melted, they can crack when the material shrinks during cooling. Thermal cameras or melt-pool sensors can help detect unusually high reheating in these areas.

Solidification cracking. Solidification cracking (also known as hot cracking) occurs while the molten metal is solidifying. As the material cools and contracts, narrow liquid films between solidifying grains can tear apart. This often depends on the alloy composition. Sudden changes in melt pool shape or brightness, visible through optical monitoring, can signal the beginning of this defect.

Delamination. Delamination occurs when one fused layer does not properly bond to the layer below it. This can happen if the laser does not penetrate enough or if residual stresses pull the layers apart. Monitoring layer height and melt pool penetration helps detect early signs of delamination, allowing the machine to modify energy input or perform a local re-scan.

3.2 In-Situ Monitoring Technologies

In-situ monitoring provides real-time information about the melt pool, powder bed, and thermal behavior during L-PBF. Each sensing method captures different physical features of the process, making them complementary. Because each sensor is sensitive to different physical behavior, combining several modalities greatly improves robustness. Optical, thermal, and photodiode signals often reveal different aspects of melt pool dynamics, and their simultaneous use reduces false detections and strengthens defect prediction.

Optical monitoring. High-speed cameras observe melt pool shape, spatter movement, and track continuity. Variations in melt pool width or brightness are strong indicators of unstable melting or lack of fusion [26].

Infrared and thermal monitoring. IR cameras and pyrometers measure melt pool temperature and cooling rates. These signals help detect overheating, insufficient penetration, or heat accumulation across layers [27].

Coaxial photodiodes. Photodiodes collect light emitted from the melt pool and plume along the laser path. Sudden intensity changes correlate with keyhole instability or plume fluctuations [28].

Acoustic emission monitoring. Acoustic sensors detect vibrations caused by cracking, delamination, or spatter impact. This technique is particularly useful for identifying internal defects not visible to optical or thermal sensors [29].

Layer-wise surface measurement. Profilometry and structured-light imaging monitor layer height, recoater streaks, or surface warping. These deviations often signal deeper problems in melt pool stability or powder spreading [30].

Together, these sensing methods provide a multimodal description of the process and support early detection of defect precursors.

3.3 Machine Learning Algorithms

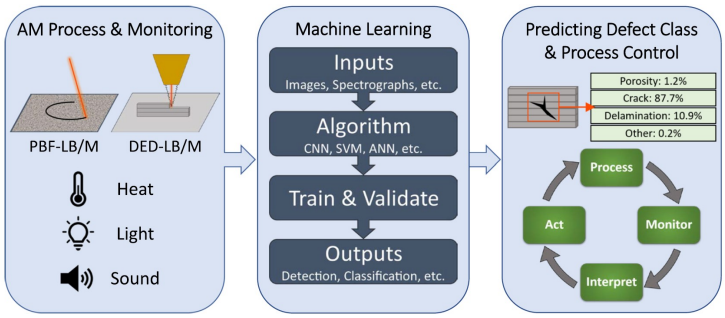

Figure 11: Overview of the integration between in-situ monitoring, machine learning, and process control in metal AM [31].

Machine learning helps interpret the large amount of complex sensor data generated during L-PBF. Because the process is highly non-linear and difficult to model physically, ML is particularly well-suited for identifying patterns related to defect formation. Figure 11 provides a high-level overview of how in-situ sensor data are processed using machine learning models and how these outputs can be used to support defect detection and closed-loop control.

Raw sensor signals are first processed into features such as melt pool width, cooling rate, plume intensity, or acoustic frequency content. Given the variety and complexity of the defect mechanisms described in Section 3.1, these feature sets capture the most relevant physical signatures that distinguish stable melting from defect-prone conditions.

Supervised ML methods (e.g., CNNs, SVMs, random forests) have been applied to identify known defect types [31], but they require large labeled datasets, which are often difficult to obtain. Even though we have described several defect types in the previous paragraphs, L-PBF processes can produce many variations and combinations of these defects, making it challenging to compile complete and reliable labels. For this reason, many studies instead use unsupervised or anomaly-detection approaches. Techniques such as autoencoders, clustering, or Gaussian mixture models learn what a "normal" process looks like and flag unexpected deviations that may indicate emerging defects [32].

Sensor fusion methods, which combine data from multiple sensors, further improve reliability. By integrating optical, thermal, and photodiode signals, ML models can better capture the different physical aspects of melt pool behavior and provide more robust defect detection [27].

3.4 Closed-Loop Control

After defects or instabilities are detected, closed-loop control can adjust process parameters during the build. These corrections typically involve modifying laser power, scan speed, hatch spacing, or performing a local re-scan.

A typical feedback loop involves: (1) extracting melt pool or anomaly metrics, (2) comparing them to target values, (3) computing the corrective action, and (4) updating the laser parameters in real time.

Photodiode-based feedback has been shown to stabilize the melt pool and reduce keyhole porosity by regulating laser power [28]. Thermal feedback systems have also been demonstrated, using melt pool temperature to tune energy input [33]. More advanced approaches, such as Bayesian optimization and model predictive control, automatically tune parameters to keep the process stable even for complex geometries [34].

3.5 Advantages and Remaining Challenges

The integration of in-situ monitoring, machine learning, and closed-loop control provides several benefits for L-PBF, but also introduces practical challenges that must be addressed for widespread industrial adoption.

Advantages.

- **Improved part quality:** Stabilizing melt pool behavior reduces porosity and leads to more consistent mechanical properties across the build.

- **Enhanced industrial readiness:** Real-time monitoring and correction bring L-PBF closer to meeting qualification requirements in aerospace, medical, and energy applications.
- **Reduced post-processing:** Detecting and correcting defects during the build decreases reliance on CT inspection, polishing, or machining.
- **Wider process windows:** Better control enables higher scan speeds, new alloy systems, and larger components with lower risk of build failure.

Remaining challenges.

- **Sensor integration and cost:** High temperatures, spatter, and metal vapor complicate long-term sensor reliability and calibration.
- **High data rates:** Optical, thermal, and acoustic sensors produce large data volumes that require fast processing for real-time use.
- **Model transferability:** ML models trained on one machine, alloy, or geometry often do not generalize well to others.
- **Explainability and certification:** Industrial standards require interpretable decisions, which can be difficult when using black-box ML methods.
- **Control stability:** Real-time parameter adjustments must be carefully tuned to avoid oscillations or overshooting during the build.

4 Wire Arc Additive Manufacturing

Written by Anastasia Meijer

Of the many AM processes for metallic component manufacturing, Directed Energy Deposition (DED) is one. DED is mainly used for larger components, and for repair, because of its higher material deposition rate [35].

One of the techniques used in DED, is Wire Arc Additive Manufacturing (WAAM). WAAM is cost-effective, produces minimal waste, and also has a lessened environmental impact. For example, WAAM is used in large structural applications. Here, WAAM can reduce fabrication time by 60%, and use 85% less energy, compared to powder-based AM processes [35].

WAAM also carries some disadvantages with it. Failure to control critical parameters, causes defects to occur in the final product. These defects are usually found in one of three categories: geometric, process-induced, and residual stress defects [35].

Multiple fields of research are developing at the moment, trying to control the critical parameters, and reducing the amount of defects. Some of these fields are MWAAM, ML Control, and the use of Digital Twins [35].

The topics named in this introduction, will be expanded upon further in this Section. The topics in this section have been selected, because of their large potential in future research and applications. But, WAAM is a far broader topic, with more roads to explore.
Some topics that are also interesting to explore, are the different metals used, other type of defects, and other possible advances in WAAM. The choice has been made to not look at metal use, as this veers heavily into materials engineering, and this Section focuses more on mechanical properties and advances. Other defects and possible advances, have not been discussed, as this does not fit into the scale of this report. The most important topics in these categories, have instead been treated with much detail.

4.1 Mechanisms of WAAM

How does WAAM work?

The basis of WAAM lays in welding technologies. MIG/GMAW, TIG/GTAW, and Plasma Arc Welding/PAW can be used in WAAM. WAAM makes use of layer by layer deposition of welding beads [36]. A metal wire is heated using an electric arc, and melts. This happens at a pool of already molten metal. Afterwards, it hardens at the melt pool's border, creating the component layer by layer [37]. The retrieved result must then be treated by build machining, in order to become smooth [36]. An overview of the general WAAM process has been illustrated in Figure 12.

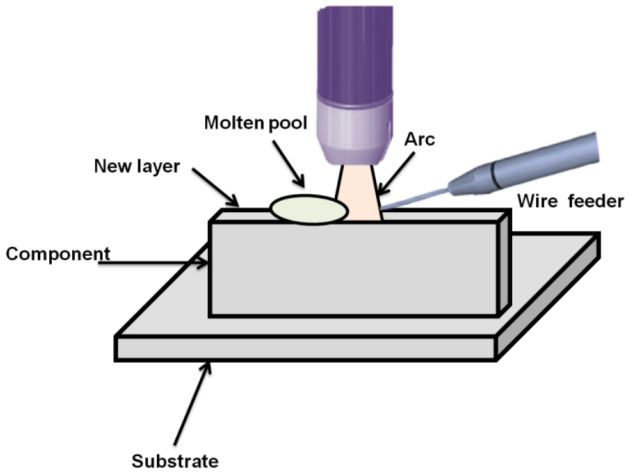

Figure 12: The WAAM technique [37].

Many materials can be used in WAAM. For example, titanium based alloys, stainless steel, nickle, bronze, and aluminum. This makes it a fairly versatile technology, to be applied in many industries [36].

Current uses

At the moment, WAAM is mostly used for large structures and repair [36]. Large scale components can be produced completely dense, with low production costs. The cost of the metal wire used in WAAM, is around 15% of how much the same amount of metal would cost in powder. This makes WAAM a relatively cheap AM process, compared to powder-based processes [37]. Lightweight construction is also achievable, by using materials such as titanium and aluminum alloys as filler material [36].

WAAM is used in a number of industries. These include the aerospace, aviation, automotive, and medical industries. In the transport sectors, the use of lighter metals is important, and can be achieved with WAAM. For aerospace, the possibility to produce complex parts from titanium and nickel alloys, but keep the cost relatively low, is interesting. And for the medical industry, the cost is important, as it's an industry that uses a lot of (single-use) products [37].

4.2 Defect types

This Section will further explain the three defect types. These are geometric, metallurgical, and process-induced defects.

Geometric defects

One of the major geometric defects in WAAM, are bead defects. As mentioned before, WAAM uses layer by layer deposition of welding beads, which are formed when welding wire melts and fuses with the base material. The different layers of beads then form the product. A bead has multiple parameters, such as height, width, radius, and degree of contact angle. When these are not adhered to accurately, or if these are not well established, then many defects can occur, both in the mechanical properties, and in the surface finish. Defects in the surface finish is called bead

waviness [38]. For example, the penetration of the bead into the base material could be insufficient. This causes the material to have weak bonds, which can later cause many mechanical problems, such as low strength of the finished product. The insufficient penetration also causes for more macroscopic defects, such as visible defects in the finished product, making the surface finish not adequate [38]. An overview of the most common geometry effects on the mechanical properties and surface finish can be found in Figure 13

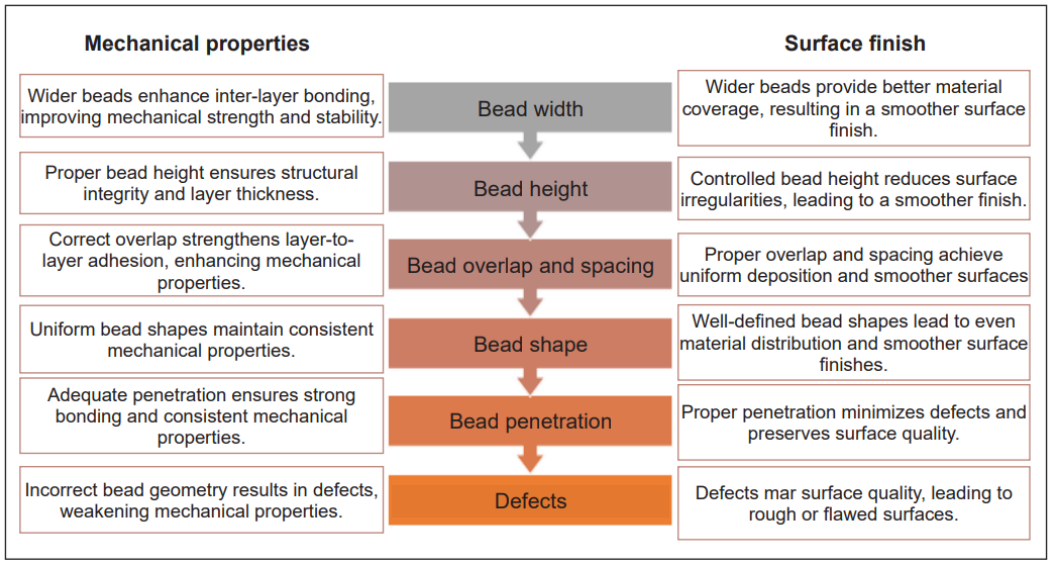

Figure 13: An overview of the most common effects on a product by bead defects [38].

Process-induced defects

A critical process defect is lack-of-fusion (LoF). LoF happens when a newly deposited layer does not bond well with the base material, or previous layers [39]. This mainly happens for two reasons. Firstly, it happens when heat is not handled correctly during the deposition process[39]. Secondly, it occurs when beads do not overlap adequately, as seen in Figure 14 [40].

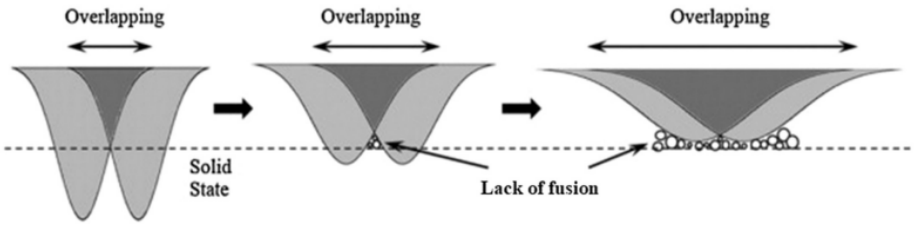

Figure 14: Lack of Fusion by incorrect overlapping [40].

Weak bonding affects the structural integrity of a product, and can lead to cracking and premature failure when loaded. Corrosion is also often more prevalent when weak bonds are present, making the product vulnerable to the environment. This all makes for unreliable, or even unusable products [39].

Residual stress defects

Residual stresses (RS) are generally defined as stresses that remain in welded objects, even without without load or thermal influence [41].

RS in WAAM are internal stresses, in the products of the WAAM process. These stresses cause premature failing, because the processes of initiation and propagation of cracks start earlier [42].

RS in WAAM are mainly caused by the cyclic heating and cooling of the component, which happens during the layer by layer deposition of the molten metal . To counter the RS, one could propose to lower the temperature during the melting process of the metal feed, since a large heat difference between deposition and cooling, increases the RS. But, a high energy input during deposition, also improves the surface quality, ductility, and deposition rates during the WAAM process. For this reason, the choice can be made to melt at a higher temperature, inducing a higher RS. To lessen this effect, the cooling process can be elongated in time, and performed with a higher heat input [42].

4.3 Advances

Three advances in the field of WAAM have been chosen to discuss in this Section. These are MWAAM, Machine Learning, and Digital Twins.

MWAAM

WAAM, in its simple form, uses a single wire feeder to melt a single wire, with an electric arc. Should one want to produce multi-material components, the wire has to be switched. This leads to increased cycle times, surface irregularities, and interruptions in the deposition process. A solution for this is Multi-Wire Arc Additive Manufacturing, or MWAAM [43].

MWAAM allows for multiple wires, made from different metals, to work as feedstock. Each of these can be fed at other speeds, allowing for specific chemical compositions in the melting pool [43]. MWAAM is far more efficient than single-wire methods. For example, Xu (2022) found that MWAAM can have an efficiency, double as high as single-wire methods. And this is possible, while maintaining appropriate mechanical properties [44].

One way to use MWAAM, is using two wires, but one twin-wire torch. Pulse programs, which decide when and long a peak in voltage will be supplied, are wired into the setup. Parameters based on wire feed speeds are determined, using data from welding databases [43]. When using dual wires, two pulse power systems, and a single torch, one can receive good results. Higher deposition rates were achieved, and gradients in the material could be created. This is interesting for load-bearing structures, which deal with unique load distributions [45].

Dual-wire welding is quite a different process than single-wire welding, making the process parameters differ slightly. This can be used to lessen the process-induced defects that are usually found withing WAAM products [43]. Using Finite Element Methods and different area-filling paths, in combination with dual-wire welding, has proven to significantly reduce thermal and residual stresses [45].

ML

To detect process-induced defects, such as lack-of-fusion (LoF), it is important to keep close watch during the deposition process. This can be done with in-situ monitoring. But key to analyzing the results observed via monitoring, is Machine Learning (ML) [46].

One optical sensor-based detection method is spectroscopy. This method is relatively inexpensive, and it can detect many defects. For example, the welding plasma's electron temperature can be observed. This makes it possible to identify many defects, one of which is LoF [47].

The classification model that is one of the most commonly used for LoF detection, is Support Vector Machine (SMV). SMV is effective in high-dimensional spaces, and non-linear problems. The biggest problem is that computation is expensive for large datasets [46].

Another use of ML in WAAM is to solve the geometric defects, namely bead geometry defects. Bead geometry can be optimized using a bio-inspired algorithm, with the most common one being a genetic algorithm (GA). GA evaluates bead geometry as a vector, represented by measured parameters of the ongoing production process. It can then predict the performance of the bead geometry with a regression model, and can give the product a fitness score [48].

Using ML in WAAM is an addition that is very interesting for its potential. One could use it to very accurately detect LoF defects, and then act accordingly. The most basic response would be to stop working on that object, saving on more resources and time that would be spend on that object. But, using it in relation to autotomized WAAM processes would be even more interesting. Combining the detection ML model with decision-making ML models, would make for the possibility for an object to have a minor defect, but to still be used. A decision-making ML model could decide the defect would be minor enough, for it still to be completed, but with some adjustments in the production process to compensate for the defect. This, however, is still a developing technique, and has not yet been demonstrated.

Digital Twin

WAAM has to do with complex behavior, especially looking at thermal behavior. This makes numerical simulations very important, as to understand how different variables influence the final product. The problem is that the computational power of numerical simulations is limited, and not real-time applicable. A solution for this is to introduce the Digital Twin (DT). A DT is a computer-generated replica of a real-world object, that can adjust together with a real-time process. They constantly analyze, and update the process [49].

Two of the earlier stated defects, bead waviness and residual stress, can be lessened by using Digital Twins. They are both caused by improper usage of heat. A Digital Twin would be able to analyze in time when there is a problem with the heat. A Digital Twin could then update the process, by sending commands to the torches to adjust the heat addition. This would solve the two earlier stated defects [49].

5 Multi-Material Metal Additive Manufacturing

Written by Agasthya Vivek

5.1 Introduction

In continuation of the theme of this report, with a focus on recent advancements in the field of additive manufacturing (AM) of metal parts, this section focuses on advancements pertaining to the use of multiple materials. AM is unique not only in its ability to produce geometrically complex parts, but in its ability to vary material properties in three dimensions in a single manufacturing step - a task that cannot be accomplished by traditional means. This allows for material properties to be tailored in three dimensions, and for the creation of functionally graded material (FGM) parts.

This section details the combinations of materials possible with metals, the processes used to manufacture multi-material parts (PBF and DED), the advantages and applications enabled by the use of multiple materials, and the challenges and potential solutions that result. Single-step co-bonding processes are focused on primarily, while topics such as in-situ alloying that are closely associated have been excluded from scope due to the heavy discussion of metallurgy associated.

5.2 Material Combinations

The primary focus of this report is on the additive manufacturing of metals. In the context of printing parts constituted of multiple materials, various combinations of metals remain of the highest interest, allowing for properties to be tailored locally. The primary challenges encountered are in the adhesion between different metals, and problems caused by different thermal properties [50]. Different cooling rates, for example, can introduce internal stresses that compromise the part. Using multiple metals with laser-based processes is also complicated by the different absorptivities exhibited by different metals [50] - a challenge potentially remedied using multiple lasers with different wavelengths.

With the versatility of powder-based processes in particular, it is also possible to use combinations of different classes of materials, such as metals and polymers, and metals and ceramics, in a single manufacturing step. The former, while of great interest to industry owing to the prevalence of assemblies containing a combination of the two, remains unfeasible to manufacture in a single step and is hence omitted from discussion. Even for sintering-based laser processes, temperatures routinely reach upwards of 700 °C [51], which can degrade even high-performance polymers like PEEK, which has a glass transition temperature of approximately 150 °C [52]. Other techniques, such as binder jetting, that avoid such high temperatures do not fully exploit the material properties of metals, but can be used to create composites of interest.

Metal-ceramic parts represent a marriage of toughness with high hardness and wear resistance. The high-temperature strength and corrosion resistance of ceramics can also be leveraged, making this material combination one of great interest. While the gap in thermal properties is not always as extreme as that between metals and polymers, it does still present significant challenges. With certain combinations, ceramic flow temperatures can even be higher than the metal's evaporation temperature [50].

5.3 Processes

Laser powder bed fusion (L-PBF) and direct energy deposition (DED) have been discussed in detail in the prior sections and hold the greatest promise in enabling the production of multi-material components. Commercially available equipment is currently tailored to production with a single material, but similar designs with modifications are feasible to use multiple materials.

5.3.1 Direct Energy Deposition (DED)

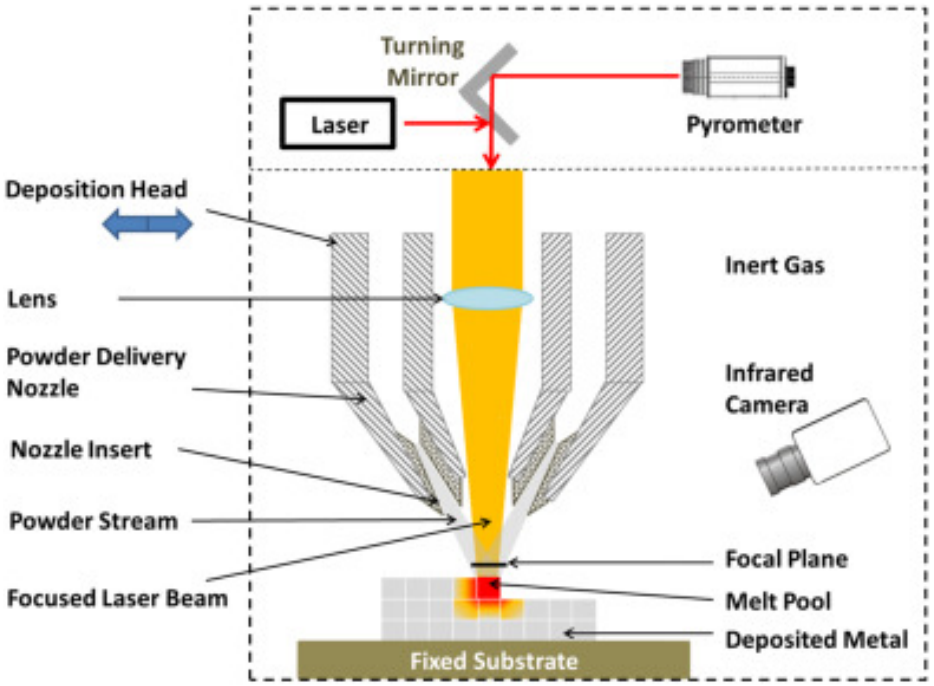

Figure 15: MMAM Powder Based DED [53].

Direct energy deposition using a laser uses the same process mechanics as WAAM described in Section 4. A laser substitutes an electrical arc to create a melt pool into which material is supplied either as a powder via actuators or fed as a wire feedstock. Multiple powder feedstocks can be incorporated with ease into this manufacturing process using multiple powder delivery nozzles, as seen in Figure 15, which uses inert gas to control powder delivery while avoiding corrosion and contamination of the part [53].

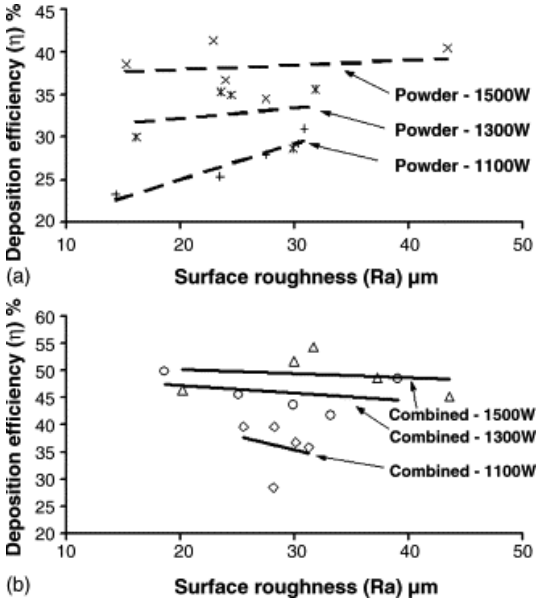

Figure 16: Deposition efficiency vs Surface roughness for wire+powder DED [54].

Using a wire-based feedstock also allows for multi-material additive manufacturing (MMAM) parts using multiple wire feeders. It provides minimal constraints when working with different combinations of metals, as most can be drawn into wires, but challenges arise if combinations of metals and ceramics, or other such materials that are not drawable, are intended for use in the part [50]. Wire feeders also tend to be bulkier than powder delivery systems, placing restrictions on the number that can be accommodated in the machinery.

A hybrid approach using a combination of the two techniques has been shown to have promise. It was shown to have 20–25% less porosity than a purely powder-based approach and greater deposition efficiency with the same laser power supplied. In addition, as seen in Figure 16, the surface roughness reduces with deposition efficiency with the combined approach, in contrast to the increase observed when using only powders [54], allowing for better part quality.

With both powder and wire approaches, the amount of each metal dispensed is varied as the melt pool moves across the layer, controlling the composition within the layer as well for true three-dimensional material property control. DED has been demonstrated to produce high-quality multi-material parts almost devoid of porosity, suitable for both medical and structural applications, highlighting its feasibility.

5.3.2 Laser Powder Bed Fusion (L-PBF)

The mechanism of L-PBF, detailed extensively in Sections 2 and 3, is ideal for MMAM. As each step involves adding a layer of powder and then sintering/melting the required regions with a laser, one or more additional materials can be incorporated into the part by controlling where each material is deposited on each layer. It allows the greatest versatility in the combination of materials possible, as powder feedstocks are available for ceramics and other materials as well. A variety of approaches are highlighted in Figure 17.

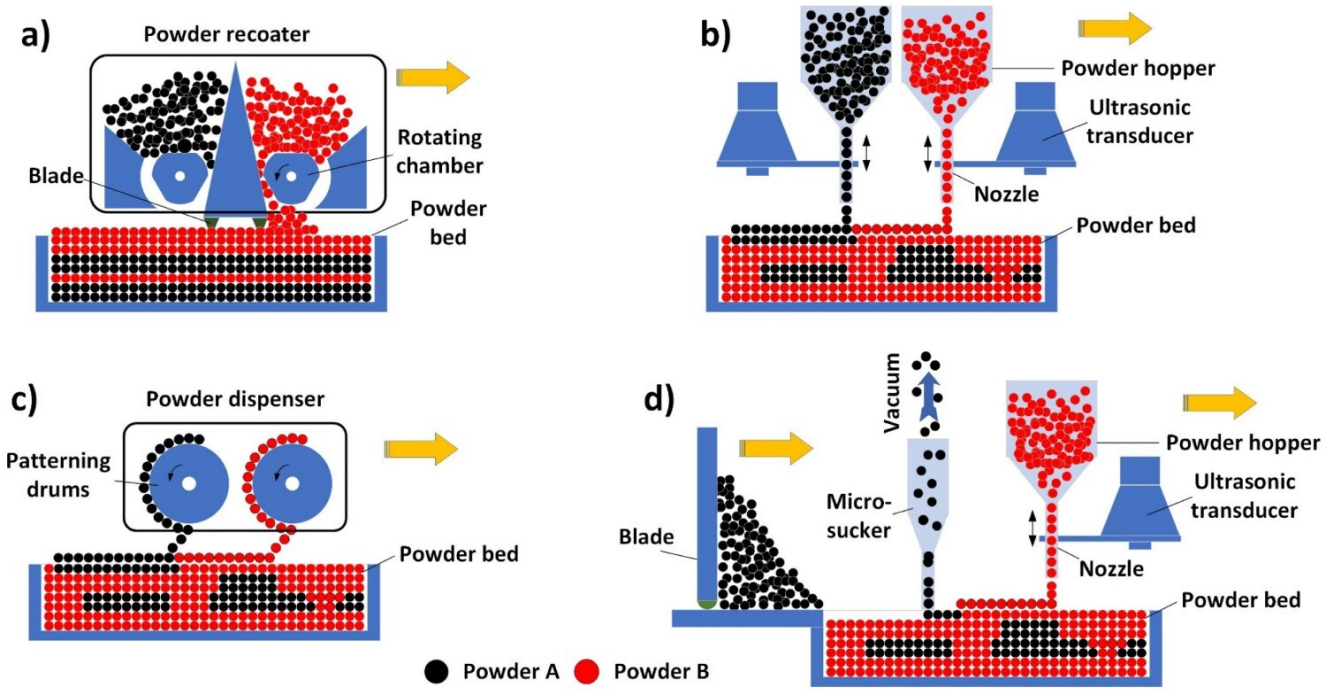

Figure 17: MMAM L-PBF strategies [55].

Using two separate powder containers, as seen in Figure 17A, is one of the easiest approaches, but allows for only one material per layer, resulting in material variation only in one dimension and in further restrictions on part design [55]. This can be worked around by sintering a section of the layer with the first material, using a vacuum or electrostatic removal to remove unsintered powder, and then filling the remainder of the layer with the second material for a second sintering operation [56]. While simplicity is an advantage, this approach doubles recoating time per layer in addition to the time taken for powder removal, while increasing the likelihood of contamination of unsintered powder from residues of the second material.

Ultrasonic actuators paired with multiple materials enable multiple materials within the same layer by depositing them with micron-scale precision, as seen in Figure 17B. Recoat time is unchanged, and no time is spent on material removal, but inconsistencies in layer thickness remain a problem here [55].

Figure 17C highlights an approach based on a similar mechanism to laser printers, albeit using suction in place of electrostatic attraction. Two drums have internal suction applied through a mesh in the areas corresponding to material location on the layer. Suction is selectively switched off as the cylinder rotates to create the desired layer, albeit with the potential for layer contamination from unintended powder discharge off the cylinder [55].

Various aspects of the techniques can be combined together, as in Figure 17D, where ultrasonic actuators are combined with vacuum-based material removal and conventional layer deposition techniques, allowing for a large variety of materials to be used, with up to six actuators and powder stores demonstrated [55].

In metal–metal applications, these techniques maintain the relatively high tolerances of L-PBF, with less than 0.1 mm of dimensional error observed in the creation of CuSn10/4340 steel parts [57]. Precise control over material properties within the part is possible in this regard, and machining steps that would be required for the same tolerances following the welding of two

dissimilar materials are not required.

While the characteristics and advantages of DED and PBF have been discussed in other sections, in the context of MMAM both have demonstrated the ability to produce high-quality parts with metals. Material properties might vary, however, as the different temperatures and process mechanics can result in different metallurgies with the larger array of phases present in a multi-metal system [58].

5.4 Advantages and Applications

MMAM techniques build upon the existing advantages of additive manufacturing. Along with complex geometries, they enable the production of functionally graded materials and parts that would conventionally require multiple steps in a single step. Greater design flexibility follows from this, allowing for better performance and reduced weight as part assemblies are combined into a single part. In comparison to multi-step procedures, the build time is shortened, the cost of fasteners and assembly labour is eliminated, and material wastage is minimised, presenting cost benefits [59]. Through the use of multiple materials, corrosion resistance can be improved, toughness and wear resistance can be instilled together, electrical conductivity can be tailored, biocompatibility can be ensured, and negative coefficients of thermal expansion can be created in the part.

A myriad of potential applications stem from these possibilities. In jewellery, it could enable intricate designs with multiple precious metals. In electronics, through the use of metals with ceramics as an insulating material, embedded circuits can be incorporated into parts. It could also be a good fit for the nuclear industry - parts made from copper with a tungsten outer layer would have high-temperature resistance and plasma resistance, with more efficient cooling due to copper's high thermal conductivity [60].

It is particularly promising for use in the aerospace sector. Inconel alloys, which have found use in turbine components for their high-temperature properties, have been used as a part of bimetallic MMAM parts with the final parts devoid of cracking and with low porosity. Separate trials have combined Inconel 718 with copper alloys to improve thermal diffusivity by 250% [59]. By enabling better cooling, if implemented, this could allow for higher temperatures within jet engines, consequently improving their efficiency. Parts constituting Inconel 718 paired with 316L stainless steel also demonstrate versatility across a large temperature range, maintaining strength and toughness at lower temperatures, with oxidation resistance and high-temperature resistance [57].

The ability to use one metal for structural purposes and another on the exterior to add biocompatibility makes this a key technology for medical implants. Titanium implants could be finished with various external layers for different intended effects. The shape-memory properties of NiTi can be used to induce bone growth around the implant [61], while Cu–Ti alloys can improve the anti-bacterial properties around the implant [62].

The stiffness of the femur is approximately 1.9 GPa [63], while that of Ti6Al4V (a commonly used alloy in implants) is approximately 110 GPa [64]. This large difference results in implants shielding the bone they are embedded into from stress, which gradually results in implant loosening. Functionally grading titanium implants could allow them to match the material properties of the surrounding bone more closely to avoid this issue [62].

5.5 Challenges and Solutions

As with the advantages of MMAM, it is constrained in the same ways the underlying AM processes are. Tolerances rivalling machining cannot be reached, production rates may not compare to conventional processes, and surface finishes may not be optimal [50].

5.5.1 L-PBF-Specific Issues

In Section 17, contamination of the print layers with different materials was listed as a concern. Contamination of the unmelted/unsintered powders in a similar manner is another detrimental aspect of MMAM, as it undermines the low material wastage AM is known for by complicating the re-use of remaining powder, increasing costs [57]. Separation techniques based on powder size or varying magnetic properties have been proposed, but in the context of metal–metal parts where powder sizes are often similar and multiple metals may not respond to magnetic fields, efficiency is limited.

Porosity can also be a problem when ultrasonic actuators are used for multiple metals, with no compaction of the layer performed [55].

5.5.2 DED-Specific Issues

When using multiple metals, cracks, pores, delamination, and unmelted powder particles are encountered more frequently. Residual stresses from the process have also been found to concentrate in the metal with a lower coefficient of thermal expansion [57]. Furthermore, discrete transitions between materials can cause interfacial cracking and the formation of brittle intermetallic phases [55]. The fatigue life of the part suffers as a consequence of these defects. Using CALPHAD can allow for process parameters to be tuned to these intermetallic compounds, while transition zones between the two metals can also be employed. The gradient path method outlined in Figure 18 involves transitioning volume fractions from 0 % B to 100 % B over a certain distance, with bonding typically not being a problem, with the exception of cracking caused by unmelted particles and intermetallics formed. Using an intermediate section involves the use of a third metal C in between that bridges the thermal properties of metals A and B, while preventing the formation of intermetallic phases [65].

Beyond manufacturing, the novelty of MMAM provides design challenges that are still being tackled. Industry-standard STL files do not hold information on material, colour, or gradients. Newer file formats, such as the additive manufacturing file (AMF), do have these capabilities but are not yet ubiquitous [66]. This can make part design using older software packages challenging, especially in the context of implementing material gradients. G-code sent to the AM system must also be split and modified in accordance with the implementation of the various material feeding systems. For parts that feature discrete boundaries between different metals, a workaround has been devised where sections constituted of different materials are modelled and sliced separately as a part of a global assembly [67] - adding significant complexity.

For conventional manufacturing techniques and for AM techniques with a single material, a variety of software packages are available to simulate the process and optimise process parameters for optimum results. Owing to the nascent nature of multi-metal use, such tools are yet to be developed, resulting in the predominance of a “cook and look” trial-and-error-based approach, which can be time-consuming and expensive. Machine learning algorithms show early promise in this regard, with initial trials for a Cu–316L steel process allowing for the calculation of required

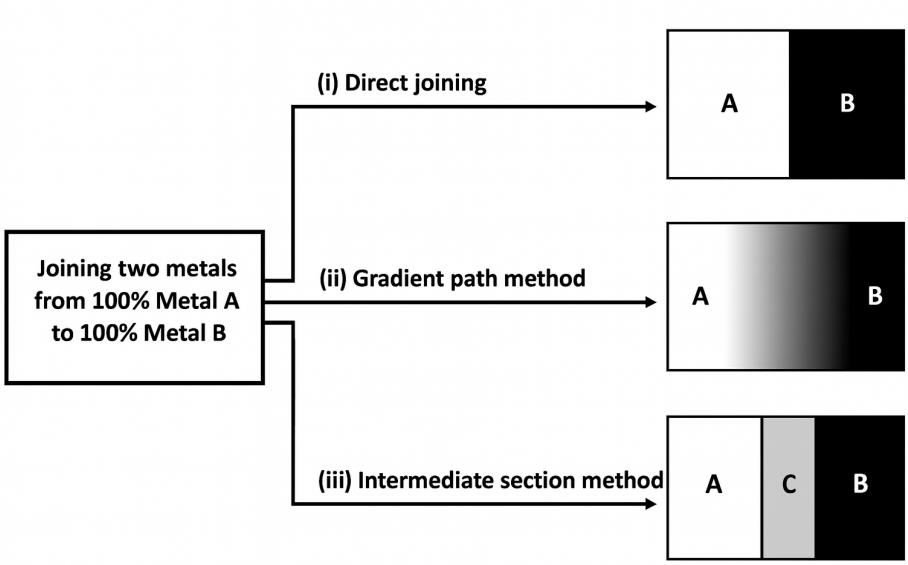

Figure 18: Material Joining Strategies [65].

L-PBF parameters based on the mass fraction of each component [68]. The primary objective is to work toward a thinner interface between the various metals, which is associated with a higher tensile strength and is achieved using a greater scan speed to reduce energy input. This also reduces melt pool temperatures and consequently the temperature gradient present, driving directional grain growth to a lesser extent to produce finer grains. Optimisation of the scan speed is necessary, as too low a scan speed can increase porosity, while high scan speeds can result in spattering [60].

6 Laser Wavelength technology

Written by Manuel Pascual

6.1 Introduction to Laser Wavelengths Used in Metal Additive Manufacturing

This section focuses on the colour (i.e., wavelength) of the laser beam. Different materials have different characteristics that affect how they interact with a laser during additive manufacturing (AM). This is the reason why a variety of laser wavelengths exist for metal processing. Both classical and modern techniques are discussed here, with greater emphasis on the latter, as they constitute the main point of the overall project. [69] [70]

6.1.1 Wavelength and Colour

There are three primary laser colours used in metal AM: infrared (IR), green, and blue. A fourth wavelength region, ultraviolet (UV), also exists but is mainly applied in microprocessing rather than metal AM.

Infrared Laser (1030–1080 nm)

This is the dominant wavelength in LPBF and DED industrial processes. It is usually generated by ytterbium-doped fibre lasers (Yb-fibre). Its widespread use stems from its high electrical efficiency, excellent beam quality, and strong industrial reliability. [71]

Green Laser (515–532 nm)

Green laser radiation is normally obtained through second-harmonic generation (SHG), where an infrared beam passes through a nonlinear crystal and part of it is converted to half the wavelength (e.g., 1064 nm to 532 nm). It is becoming increasingly relevant in AM because many metals show significantly higher absorption in the green region. [72]

Blue Laser (445–480 nm)

Recently developed high-power blue diodes have made it possible to surpass green-laser performance in highly reflective metals such as copper and precious metals.[73]

6.1.2 Absorptance Concept

The absorptance of a metal is the fraction of incoming laser energy that is converted into heat upon interacting with the metal surface. This depends on optical properties such as refractive index and electrical conductivity. Many traditional AM metals exhibit sufficient absorptance at IR wavelengths; however, highly reflective metals absorb only a small portion of the incident energy, making them difficult to process with infrared radiation.

Three main implications affect the AM process:

Energetic Efficiency Low absorption requires higher laser power to heat the metal to its melting temperature.

Thermal Stability Poor absorption leads to temperature fluctuations within the melt pool, which may result in porosity or geometric defects.

Optical Interactions Highly reflective metals can redirect part of the laser beam back into the optics, causing machine wear or damaging sensitive components. [74]

6.1.3 Processability of Metals Depending on Wavelength

The processability of a metal depends on its ability to absorb energy at the laser wavelength. Contributing factors include surface reflectivity, electronic structure, chemical composition, and oxidation state.

Figure 19 shows the spectral absorptance of several high-purity metals with cleaned, non-ideal surface finishes [**?**]. The graph demonstrates that certain metals exhibit significant drops in absorption beyond specific wavelength thresholds.

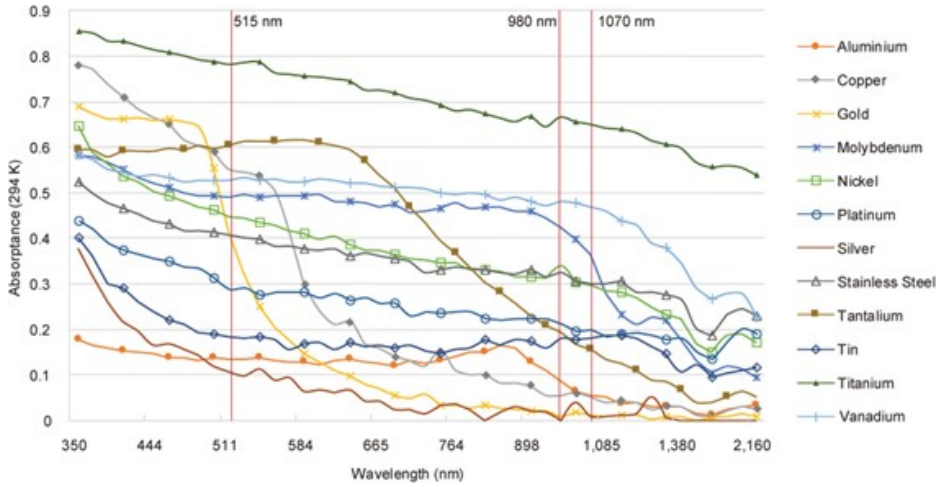

Figure 19: Spectral absorptance for various high-purity metals [].

The next table summarizes the behavior of the main metal families at different wavelengths:

Metallic Family	IR Absorption	Green Absorption	Blue Absorption
INOX Steel	High	Medium-high	Medium
Titanium	High	High	High
Nickel	High	High	High
Pure Aluminium	Low	Medium	Medium-high
Pure Copper	Very low	High	Very high
Gold/Silver	Very low	High	Very high

6.2 Classic ways to generate red, green and blue colours

These classic techniques, although now partially outdated, form the foundation of the new laser–colour-generation technologies. Understanding them at least at a superficial level is essential before introducing the modern techniques. Historically, these methods relied primarily on solid–state lasers, fibre lasers and nonlinear–optical conversion processes.

6.2.1 Infrared laser

Three classical techniques were used to generate infrared light, and some of them are still employed today in a more refined form.

Nd:YAG (Neodymium-doped Yttrium Aluminium Garnet)

One of the earliest solid–state lasers developed, with a characteristic wavelength of 1064 nm. Its radiation originates from the electronic transition of the Nd^{3+} ion inside the YAG crystalline matrix after being excited using flashlamps.

This method enabled very high–energy pulses and continuous–wave operation, producing a stable melt pool. Although largely replaced today by fibre lasers, Nd:YAG systems were used widely in industry for over two decades. —[75]

CO_2 lasers

CO_2 lasers operate at a wavelength of 10.6 µm, which is far from optimal for melting highly reflective metals. Historically, they were employed for welding and, to a lesser extent, in additive manufacturing.

Their operation is based on exciting and vibrationally energising CO_2 molecules within a gas volume. Although robust, CO_2 lasers were outclassed due to the poor absorption of metals at this wavelength and the difficulty of obtaining a well–focused beam. [76]

Ytterbium-doped fibre lasers (Yb-fibre)

Still widely used today due to decades of optimisation and extremely high efficiency. These lasers rely on the Yb^{3+} transition inside doped silica fibres, typically emitting between 1030 nm and 1080 nm. [77]

Their success is based on several factors:

- Electro–optical efficiency exceeding 30%
- Excellent beam quality
- Scalable output power without significant quality degradation
- High mechanical and thermal robustness

6.2.2 Green laser

The development of green–laser technology was originally driven by research in nonlinear optics and beam manipulation rather than metal processing.

Second Harmonic Generation (SHG)

The most widespread technique for obtaining green light. A nonlinear crystal converts part of an infrared beam into radiation of half the original wavelength — typically 1064 nm to 532 nm.

First described in the 1960s after early solid–state laser breakthroughs, SHG was initially used for welding highly reflective metals. It was only later introduced into additive manufacturing for copper and precious metals. [78]

Its main disadvantages include:

- High sensitivity to optical alignment
- Strong dependence on temperature (affecting conversion efficiency)
- Limited power reaching the melt pool in early systems, often insufficient for full fusion

6.2.3 Blue laser

Before the arrival of high–power blue diodes, two principal techniques existed:

Solid-state lasers based on Pr:YLF and Ti:Sapphire

These systems used doped crystals similar to other solid lasers, but with praseodymium (Pr^{3+}) ions. They were able to generate not only blue light, but also green and red.

However, their achievable power output was very limited, restricting applications mostly to laboratory environments.

Sum-Frequency Generation (SFG)

As the name suggests, this technique combines two different wavelengths inside a nonlinear crystal, whose frequencies add up to yield blue radiation.

Despite its flexibility, the same limitation as SHG applied: **the generated power was too low for industrial use**. Therefore, its applications remained confined to research rather than manufacturing. [79]

6.3 New Emergent Techniques

Most of the "new" techniques are in fact optimisations of classical processes designed to push performance further. Most advances in the last decade fall into this category. Still, some innovations—such as hybrid systems combining infrared and visible wavelengths—have opened unexplored possibilities by exploiting the advantages of each wavelength simultaneously. In addition, diode-based systems have become increasingly powerful thanks to continued technological improvements.

Below are the latest advances in laser wavelength technology from 2023 to the present.

6.3.1 High-Power Green Laser Technology Based on Frequency Doubling

There have been significant advancements in single-laser frequency doubling; however, several limitations remain. These include the inability of nonlinear crystals to withstand extremely high power densities, reduced efficiency at high input powers, and thermal drift effects caused by temperature changes in the crystal.

To overcome these limitations, recent research proposes combining multiple fibre laser beams into one or more nonlinear crystals. The main challenge is maintaining correct phase matching between beams. With *phase-shift combining*, this issue can be solved while obtaining additional benefits such as reduction of peak power density and improved total average power.

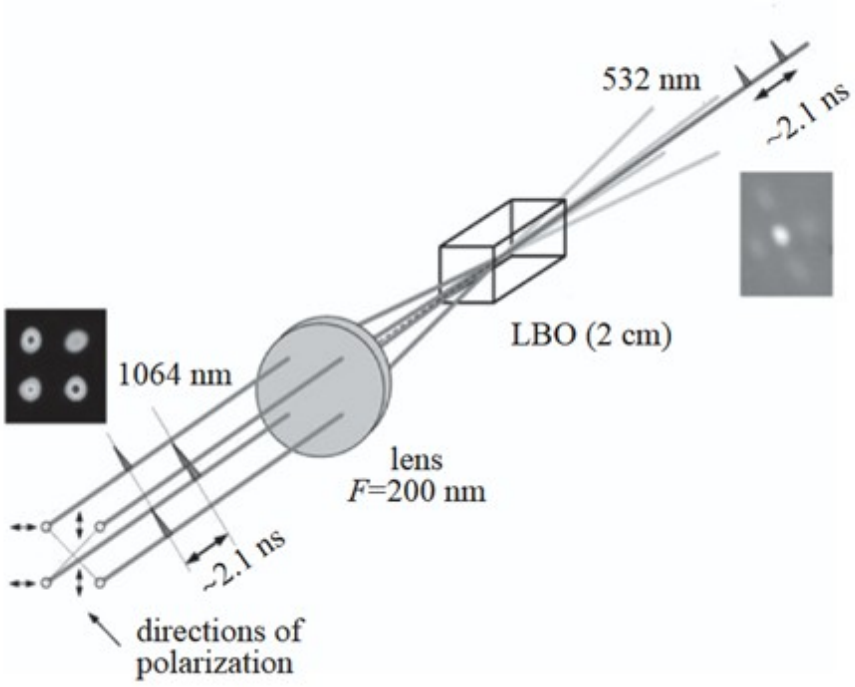

Figure 20: Multiple laser system scheme [80].

To implement this technology successfully, several key aspects must be considered:

- **High-power fibre fundamental source:** requiring narrow linewidth, excellent beam quality, stable spectral width (low-frequency variation), and stable output power.
- **Nonlinear crystal design:** typically based on LBO (lithium triborate), although BBO (beta-barium borate) or PPLN (periodically poled lithium niobate) can also be used. Critical requirements include correct phase-matching angle, adequate crystal length, good thermal conductivity, and high-quality antireflection coatings.
- **Temperature-control technology:** involving precise PID control, thermoelectric coolers, and adaptive systems. Thermal management such as conduction cooling, water cooling, and heat-sink design is essential to minimize issues such as thermal lensing or drift. [80]

6.3.2 Blue Lasers for DED

Figure 21: Laser sources LDMblue1000-40 and 1500-60 [81].

New BL-DED (Blue Laser Directed Energy Deposition) systems have recently entered industrial production. They achieve high powers, in some cases up to 10 kW, by combining individual laser diodes into diode bars. These bars are further optically combined to form a high-power beam.

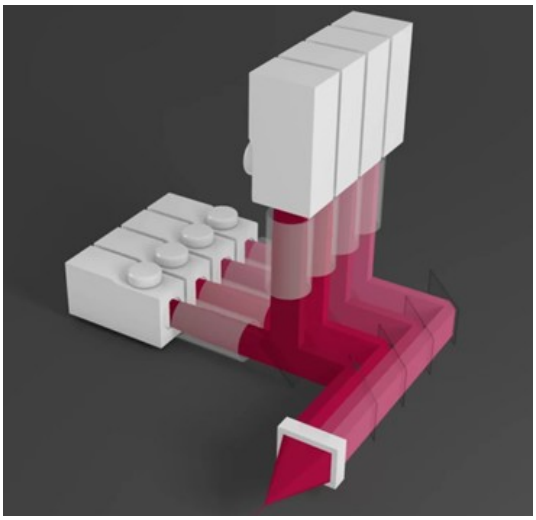

Figure 22: Stacked diodes [82].

Stacking many of these bars allows the system to scale to unprecedented power levels. The exact proprietary optical combination strategies used by manufacturers are not publicly disclosed. Nevertheless, the method is known to provide high electro-optical efficiency—often reaching 50%—a key advantage for scalability and industrial adoption.

Several research experiments have tested these high-power blue systems. One study (REF) analyzed laser performance at different power levels during welding and showed that the highest

power provided the best results. Although developed for welding, these findings are highly relevant to metal additive manufacturing. [81] [83] [82]

6.3.3 Multifrequency Laser

This technique attempts to combine multiple lasers with different wavelengths in order to harness the advantages of all simultaneously. Although functional prototypes exist at the laboratory level, industrial systems are not yet available due to limited development. Future progress in power scaling and optical optimization may make this a promising field for advanced applications. [84]

6.4 Applications

The main application of these new techniques is enabling the processing of materials that were previously difficult or impossible to work with. As discussed earlier, copper has now become a feasible option for additive manufacturing. Its thermal and electrical properties make it ideal for producing complex heat-dissipation structures or electrical components. When combined with high-density AM techniques, these properties enable superior performance compared to traditionally manufactured parts.

Significant applications include:

6.4.1 Aerospace Industry

In aerospace, both weight reduction and thermal management are critical. The ability to print high-thermal-conductivity materials such as copper opens new opportunities for creating optimised heat-transfer components and novel designs for engine subsystems where extreme thermal loads occur. [85]

6.4.2 Electric Vehicle Technology

Advanced electric vehicle systems benefit from materials with high thermal conductivity and electrical performance. New green and blue laser techniques make it possible to fabricate components such as busbars, inductors, and cooling structures using materials that were previously inaccessible through AM. [81]

6.4.3 In-Situ Alloying

High-power visible-wavelength lasers not only process highly reflective metals but can also work on conventional ones. This allows for in-situ alloying, enabling the creation of novel material combinations that were not previously manufacturable. The flexibility of blue and green AM systems opens new horizons for multi-material design and functional integration.

7 Conclusion

Metal additive manufacturing is advancing rapidly through improvements to established processes such as L-PBF and WAAM, alongside the emergence of multi-material capabilities. Across these areas, a common trend is clear: progress increasingly depends on better control of the process through sensing, modeling, and data-driven optimization. Innovations such as new alloy systems, advanced scan strategies, thermal and acoustic monitoring, machine-learning-based defect prediction, and digital twins all contribute to greater reliability and broader industrial applicability.

Although many of these approaches are still in development, they collectively indicate a shift toward more predictive, intelligent, and integrated metal AM systems. As sensing technologies mature and computational tools become more accessible, metal AM is poised to transition from parameter-driven fabrication to truly adaptive manufacturing.

References

[1] Chu Lun Alex Leung, Sebastian Marussi, Michael Towrie, Jesus del Val Garcia, Robert C. Atwood, Andrew J. Bodey, Julian R. Jones, Philip J. Withers, and Peter D. Lee. Laser-matter interactions in additive manufacturing of stainless steel ss316l and 13-93 bioactive glass revealed by in situ x-ray imaging. *Additive Manufacturing*, 24:647–657, 2018.

[2] Christian Leinenbach. Mse-422 – advanced metallurgy : 9 – high entropy alloys and bulk metallic glasses. PowerPoint presentation, 2024. Moodle, EPFL.

[3] C. Han, Q. Fang, Y. Shi, S. B. Tor, C. K. Chua, and K. Zhou. Recent advances on high-entropy alloys for 3d printing. *Advanced Materials*, 32:903855, 2020.

[4] P. D. Niu, R. D. Li, T. C. Yuan, S. Y. Zhu, C. Chen, M. B. Wang, and L. Huang. Microstructures and properties of an equimolar alcocrfeni high entropy alloy printed by selective laser melting. *Intermetallics*, 104:24–32, 2019.

[5] P. Agrawal, S. Thapliyal, S. S. Nene, R. S. Mishra, B. A. McWilliams, and K. C. Cho. Excellent strength-ductility synergy in metastable high entropy alloy by laser powder bed additive manufacturing. *Additive Manufacturing*, 32:101098, 2020.

[6] H. Z. Lu, C. Yang, X. Luo, H. W. Ma, B. Song, Y. Y. Li, and L. C. Zhang. Ultrahigh-performance tini shape memory alloy by 4d printing. *Materials Science and Engineering: A*, 763:138166, 2019.

[7] S. L. Sing and W. Y. Yeong. Laser powder bed fusion for metal additive manufacturing: perspectives on recent developments. *Virtual and Physical Prototyping*, 15(3):359–370, 2020.

[8] Z. Xiong, P. Zhang, C. Tan, D. Dong, W. Ma, and K. Yu. Selective laser melting and remelting of pure tungsten. *Advanced Engineering Materials*, 22(5):1901352, 2020.

[9] Wenhui Yu, Swee Leong Sing, Chee Kai Chua, and Xuelei Tian. Influence of re-melting on surface roughness and porosity of alsi10mg parts fabricated by selective laser melting. *Journal of Alloys and Compounds*, 792:574–581, 2019.

[10] Yingli Li, Kun Zhou, Pengfei Tan, Shu Beng Tor, Chee Kai Chua, and Kah Fai Leong. Modeling temperature and residual stress fields in selective laser melting. *International Journal of Mechanical Sciences*, 136:24–35, 2018.

[11] Y. C. Wang, L. M. Lei, L. Shi, H. Y. Wan, F. Liang, and G. P. Zhang. Scanning strategy dependent tensile properties of selective laser melted gh4169. *Materials Science and Engineering: A*, 788:139616, 2020.

[12] H. Wong, K. Dawson, G. A. Ravi, et al. Multi-laser powder bed fusion benchmarking—initial trials with inconel 625. *The International Journal of Advanced Manufacturing Technology*, 105:2891–2906, 2019.

[13] Chun-Yu Tsai, Chung-Wei Cheng, An-Chen Lee, and Mi-Ching Tsai. Synchronized multi-spot scanning strategies for the laser powder bed fusion process. *Additive Manufacturing*, 27:1–7, 2019.

[14] Xiaobing Zhang, Bo Cheng, and Charles Tuffile. Simulation study of the spatter removal process and optimization design of gas flow system in laser powder bed fusion. *Additive Manufacturing*, 32:101049, 2020.

[15] Camille Pauzon, Pierre Forêt, Eduard Hryha, Tanja Arunprasad, and Lars Nyborg. Argon-helium mixtures as laser-powder bed fusion atmospheres: Towards increased build rate of ti-6al-4v. *Journal of Materials Processing Technology*, 279:116555, 2020.

[16] P. E. Carrion, A. Soltani-Tehrani, N. Phan, et al. Powder recycling effects on the tensile and fatigue behavior of additively manufactured ti-6al-4v parts. *JOM*, 71:963–973, 2019.

[17] Austin T. Sutton, Caitlin S. Kriewall, Sreekar Karnati, Ming C. Leu, and Joseph W. Newkirk. Characterization of aisi 304l stainless steel powder recycled in the laser powder-bed fusion process. *Additive Manufacturing*, 32:100981, 2020.

[18] L. Cordova, M. Campos, and T. Tinga. Revealing the effects of powder reuse for selective laser melting by powder characterization. *JOM*, 71:1062–1072, 2019.

[19] Di Wang, Guangzhao Ye, Wenhao Dou, Mingkang Zhang, Yongqiang Yang, Shuzhen Mai, and Yang Liu. Influence of spatter particles contamination on densification behavior and tensile properties of cocrw manufactured by selective laser melting. *Optics & Laser Technology*, 121:105678, 2020.

[20] T. Koushik, H. Shen, W. H. Kan, M. Gao, J. Yi, C. Ma, S. C. V. Lim, L. N. S. Chiu, and A. Huang. Effective ti-6al-4v powder recycling in lpbf additive manufacturing considering powder history. *Sustainability*, 15(21):15582, 2023.

[21] D. Guillen, S. Wahlquist, and A. Ali. Critical review of lpbf metal print defects detection: Roles of selective sensing technology. *Appl. Sci.*, 14(15):6718, 2024.

[22] E. Louvis, P. Fox, and C. Sutcliffe. Selective laser melting of aluminium components. *Journal of Materials Processing Technology*, 211(2):275–284, 2011.

[23] S. A. Khairallah, A. T. Anderson, A. Rubenchik, and W. E. King. Laser powder-bed fusion process: physics of melt pool dynamics. *Acta Materialia*, 108:36–45, 2016.

[24] W. E. et al. King. Observation of keyhole-mode laser melting in laser powder-bed fusion. *Journal of Materials Processing Technology*, 214:2915–2925, 2015.

[25] H. Gong, K. Rafi, T. Starr, and B. Stucker. Analysis of defect generation in ti-6al-4v parts made using powder bed fusion additive manufacturing processes. *Additive Manufacturing*, 1:87–98, 2014.

[26] T. Craeghs, F. Bechmann, S. Berumen, and J. P. Kruth. Online quality control of selective laser melting. *Physics Procedia*, 5:505–514, 2010.

[27] Holger Baumgartl, Jan Tomas, Ralf Buettner, and Manuel Merkel. A deep learning-based model for defect detection in laser powder-bed fusion using in-situ thermographic monitoring. *Progress in Additive Manufacturing*, 5:277–285, 2020.

[28] M. Grasso and B. Colosimo. In-situ monitoring of laser powder bed fusion. *Additive Manufacturing*, 16:1–14, 2017.

[29] S. A. Shevchik, G. Masinelli, C. Kenel, C. Leinenbach, and K. Wasmer. Deep learning for in situ and real-time quality monitoring in additive manufacturing using acoustic emission. *IEEE Transactions on Industrial Informatics*, 15(9):5194–5203, 2019.

[30] Christopher L.A. Leung, Stefano Marussi, Robert C. Atwood, Michael Towrie, Philip J. Withers, and Peter D. Lee. In situ x-ray imaging of defect formation in laser powder-bed fusion additive manufacturing. *Nature Communications*, 9(1):1355, 2018.

[31] T. Herzog, M. Brandt, A. Trinchi, A. Sola, and A. Molotnikov. Process monitoring and machine learning for defect detection in laser-based metal additive manufacturing. *Journal of Intelligent Manufacturing*, 35:1407–1437, 2024.

[32] L. Scime and J. Beuth. Anomaly detection and classification in a laser powder bed additive manufacturing process using a trained computer vision algorithm. *Additive Manufacturing*, 19:114–126, 2018.

[33] Yufeng Lai, Minh Anh Luan Phan, Chengxi Zhu, Matthew M. J. Davies, George Maddison, Matthew J. Hobbs, Iain Todd, and Jon R. Willmott. In-situ thermal imaging of laser powder bed fusion: Investigating the influence of preheating temperatures on cooling rates and melt pool dynamics. *SSRN Preprint*, 2023.

[34] Lequn Chen, Guijun Bi, Xiling Yao, Jinlong Su, Chaolin Tan, Wenhe Feng, Michalis Benakis, Youxiang Chew, and Seung Ki Moon. In-situ process monitoring and adaptive quality enhancement in laser additive manufacturing: a critical review. *arXiv Preprint*, 2024.

[35] S. Gain and D. Veeman. A review on advances and challenges in wire arc additive manufacturing: Process parameters, microstructural evolution and material performance across alloys. *Journal of Alloys and Compounds*, 1029, 2025.

[36] M. Chaturvedi, E. Scutelnicu, C. C. Rusu, L. R. Mistodie, D. Mihailescu, and A. V. Subbiah. Wire arc additive manufacturing: Review on recent findings and challenges in industrial applications and materials characterization. *Metals*, 11(6):939, 2025.

[37] R. K. Singha, K. Venkadeshwaranb, B. P. Singhc, and G. K. Kantak. Assessing the pros and cons of wire-arc additive manufacturing for material production. *MalquePublishing*, 2024.

[38] Z. K. Wani and A. B. Abdullah. Bead geometry control in wire arc additive manufactured profile - a review. *Pertanika Journal of Science and Technology*, 32(2):917–942, 2024.

[39] S.K. Polamuri, S. Chitral, and M.K. et al Adapa. A strategic approach to minimize lack of fusion defects in wire arc additive manufacturing. *Prog Addit Manuf*, 10:6965–6980, 2025.

[40] Y. Cai, J. Xiong, H. Chen, and G. Zhang. A review of in-situ monitoring and process control system in metal-based laser additive manufacturing. *Journal of Manufacturing Systems*, 70:309–326, 2023.

[41] The Welding Institute. What is residual stress?

[42] F. D. Gurmesa, H. G. Lemu, Y. W. Adugna, and M. D. Harsibo. Residual stresses in wire arc additive manufacturing products and their measurement techniques: A systematic review. *Applied Mechanics*, 5(3):420–449, 2024.

[43] R. T. Tanwar and S. Jhavar. Multi-wire additive manufacturing: A comprehensive review on materials, microstructure, methodological advances, and applications. *Engineering*, 26(4), 2024.

[44] T. Xu, M. Zhang, J. Wang, T. Lu, S. Ma, and C. Liu. Research on high efficiency deposition method of titanium alloy based on double-hot-wire arc additive manufacturing and heat treatment. *Journal of Manufacturing Processes*, 79:60–69, 2022.

[45] S. Suryakumar and M.A. Somashekara. Manufacturing of functionally gradient materials by using weld-deposition. *Proceedings of the 1st International Joint Symposium on Joining and Welding*, pages 505–508, 2013.

[46] G. Kishor, K. K. Mugada, and R. P. Mahto. Sensor-integrated data acquisition and machine learning implementation for process control and defect detection in wire arc-based metal additive manufacturing. *Precision Engineering*, 95:163–187, 2025.

[47] A. Ancona, T. Maggipinto, V. Spagnolo, M. Ferrara, and Lugara P. M. Optical sensor for real-time weld defect detection. *Sensors and Camera Systems for Scientific, Industrial, and Digital Photography Applications*, 4669, 2002.

[48] G. Mattera, S.P. Chozaki, and J. Norrish. Advances in machine learning for parameters optimisation and in-situ monitoring of wire arc additive manufacturing. *Weld World*, 2025.

[49] R. Tryhubov and M. Kryshchuk. Numerical modeling and digital twins in wire arc additive manufacturing. *Mech. Adv. Technol.*, 9(3):357–371, 2025.

[50] Amit Bandyopadhyay and Bryan Heer. Additive manufacturing of multi-material structures. *Materials Science and Engineering: R: Reports*, 129:1–16, July 2018.

[51] P. Fischer, M. Locher, V. Romano, H. P. Weber, S. Kolossov, and R. Glardon. Temperature measurements during selective laser sintering of titanium powder. *International Journal of Machine Tools and Manufacture*, 44(12):1293–1296, October 2004.

[52] Xue-Jie Liu, Mengyu Xiao, Wenjie Huang, Xing Yang, and Jun-Wei Zha. Overview of High-Temperature Polymers. In Jun-Wei Zha and Zhi-Min Dang, editors, *High Temperature Polymer Dielectrics*, pages 1–19. Wiley, 1 edition, March 2024.

[53] Scott M. Thompson, Linkan Bian, Nima Shamsaei, and Aref Yadollahi. An overview of Direct Laser Deposition for additive manufacturing; Part I: Transport phenomena, modeling and diagnostics. *Additive Manufacturing*, 8:36–62, October 2015.

[54] Waheed Ul Haq Syed, Andrew J. Pinkerton, and Lin Li. Combining wire and coaxial powder feeding in laser direct metal deposition for rapid prototyping. *Applied Surface Science*, 252(13):4803–4808, April 2006.

[55] Chao Wei and Lin Li. Recent progress and scientific challenges in multi-material additive manufacturing via laser-based powder bed fusion. *Virtual and Physical Prototyping*, 16(3):347–371, May 2021. Publisher: Taylor & Francis _eprint: https://doi.org/10.1080/17452759.2021.1928520.

[56] K. Lappo, B. Jackson, Kristin Wood, David Bourell, and Joseph Beaman. Discrete multiple material selective laser sintering (m2sls): Experimental study of part processing. 08 2003.

[57] Di Wang, Linqing Liu, Guowei Deng, Cheng Deng, Yuchao Bai, Yongqiang Yang, Weihui Wu, Jie Chen, Yang Liu, Yonggang Wang, Xin Lin, and Changjun Han. Recent progress on additive manufacturing of multi-material structures with laser powder bed fusion. *Virtual and Physical Prototyping*, 17(2):329–365, April 2022. Publisher: Taylor & Francis _eprint: https://doi.org/10.1080/17452759.2022.2028343.

[58] Daniela Medová, Anna Knaislová, Angelina Strakosova, Orsolya Molnárová, Jaroslav Čapek, Ilona Voňavková, and Dalibor Vojtěch. Comparison of direct energy deposition and powder bed fusion technology in the preparation of Ti–6Al–4V alloy. *Journal of Materials Research and Technology*, 35:3825–3840, March 2025.

[59] Ayush Verma, Angshuman Kapil, Damjan Klobčar, and Abhay Sharma. A Review on Multiplicity in Multi-Material Additive Manufacturing: Process, Capability, Scale, and Structure. *Materials*, 16(15):5246, January 2023. Publisher: Multidisciplinary Digital Publishing Institute.

[60] Chao Wei, Zhizhou Zhang, Dongxu Cheng, Zhe Sun, Menghui Zhu, and Lin Li. An overview of laser-based multiple metallic material additive manufacturing: from macro- to micro-scales. *International Journal of Extreme Manufacturing*, 3(1):012003, December 2020. Publisher: IOP Publishing.

[61] Cheng Zhu, Hawi B. Gemeda, Eric B. Duoss, and Christopher M. Spadaccini. Toward Multiscale, Multimaterial 3D Printing. *Advanced Materials*, 36(34):2314204, August 2024. Publisher: John Wiley & Sons, Ltd.

[62] S. L. Sing, S. Huang, G. D. Goh, G. L. Goh, C. F. Tey, J. H. K. Tan, and W. Y. Yeong. Emerging metallic systems for additive manufacturing: *In-situ* alloying and multi-metal processing in laser powder bed fusion. *Progress in Materials Science*, 119:100795, June 2021.

[63] M. Cuppone, B. B. Seedhom, E. Berry, and A. E. Ostell. The longitudinal Young's modulus of cortical bone in the midshaft of human femur and its correlation with CT scanning data. *Calcified Tissue International*, 74(3):302–309, March 2004.

[64] Properties: Titanium Alloys - Ti6Al4V Grade 5.

[65] Lei Yan, Yitao Chen, and Frank Liou. Additive manufacturing of functionally graded metallic materials using laser metal deposition. *Additive Manufacturing*, 31:100901, January 2020.

[66] Xiaoyu Zheng, Christopher Williams, Christopher M. Spadaccini, and Kristina Shea. Perspectives on multi-material additive manufacturing. *Journal of Materials Research*, 36(18):3549–3557, September 2021.

[67] Chao Wei, Lin Li, Xiaoji Zhang, and Yuan-Hui Chueh. 3D printing of multiple metallic materials via modified selective laser melting. *CIRP Annals*, 67(1):245–248, January 2018.

[68] Behzad Rankouhi, Salman Jahani, Frank E. Pfefferkorn, and Dan J. Thoma. Compositional grading of a 316L-Cu multi-material part using machine learning for the determination of selective laser melting process parameters. *Additive Manufacturing*, 38:101836, February 2021.

[69] Ralph Delmdahl. Trends and advances in UV-laser microprocessing. In *International Congress on Applications of Lasers &amp Electro-Optics*. Laser Institute of America, 2011.

[70] C. A. Walsh et al. Reflectivity challenges in laser-based metal processing. *International Journal of Advanced Manufacturing Technology*, 2022.

[71] Ian Gibson, David Rosen, Brent Stucker, and Mahyar Khorasani. *Additive manufacturing technologies*. Springer, Germany, November 2020. Publisher Copyright: © Springer Nature Switzerland AG 2021.

[72] J. Schoop et al. Green laser powder bed fusion of pure copper. *Additive Manufacturing*, 2024.

[73] ZHANG Jiye, WANG Jingbo, ZHANG Jun, PENG Hangyu, CHEN Lei, YANG Ying, WANG Zhihao, ZHANG Chunlin, and Wang Lijun. High power blue diode laser source for material processing. *Chinese Journal of Luminescence*, 44:1308–1314, 01 2023.

[74] Benedikt Brandau, Adrien Da Silva, Christoph Wilsnack, Frank Brueckner, and Alexander FH Kaplan. Absorbance study of powder conditions for laser additive manufacturing. *Materials & Design*, 216:110591, 2022.

[75] W. Steen and J. Mazumder. *Laser Material Processing*. Springer, 2010.

[76] J. F. Ready. *Industrial Applications of Lasers*. Academic Press, 2001.

[77] J. Limpert et al. High-power fiber lasers. *IEEE Journal of Selected Topics in Quantum Electronics*, 18(1):275–300, 2012.

[78] P. A. Franken, A. E. Hill, C. W. Peters, and G. Weinreich. Generation of optical harmonics. *Physical Review Letters*, 7:118–119, 1961.

[79] D. S. Pereira et al. Blue emission in pr:ylf solid-state lasers. *Journal of Applied Physics*, 92:2020–2025, 2002.

[80] Tian Ma, Fuquan Li, and Honghuan Lin. Recent progress of high power green laser based on frequency doubling technology for fiber laser. *Optics and Laser Technology*, 2023. PDF provided by user.

[81] Thomas Molitor Markus Rütering Simon W. Britten*, Laurens Schmid. Advances in metal additive manufacturing. *Additive Manufacturing*, 2020.

[82] Laserline GmbH. High-power diode lasers, 2025.

[83] Zhenyang Gao Huihui Yang An Wang Le Wan Cheng Luoc Yi Wu Haowei Wang Zijue Tanga, Qianglong Wei and Hongze Wanga. Novel process additive manufacturing: A review. *International Journal of Advanced Manufacturing Technology*, 2022.

[84] Fraunhofer Institute. High-power green laser research, 2025.

[85] Fraunhofer IWS. Green lasers enable additive manufacturing of pure copper. https://www.iws.fraunhofer.de/en/newsandmedia/press_releases/2020/presseinformation_2020-07.html, 2020. Accessed: 2025-11-26.